RSC Advances

PAPER

View Article Online
View Journal | View Issue

Cite this: *RSC Adv.*, 2020, **10**, 1679

The oxidation of (−)-epigallocatechin-3-gallate inhibits T-cell acute lymphoblastic leukemia cell line HPB-ALL *via* the regulation of Notch1 expression

Yu-Na Wang,†[a] Jing Wang,†[a] Hao-Nan Yang,[a] Bang-Lei Zhang,[a] Pan Zhang,[a] Pei-Yuan Sun,[a] Nin Zhang,[a] Ya Wang,[a] Jun Sheng,*[ac] Xuan-Jun Wang*[abc] and Cheng-Ting Zi *[ab]

T-cell acute lymphoblastic leukemia (T-ALL) is an aggressive hematological malignancy, and commonly associated with activating mutations in the Notch1 pathway. (−)-Epigallocatechin-3-gallate (EGCG) is the most abundant and active catechin and has been shown to regulate Notch signaling. Taking into account the highly oxidizable and unstable of EGCG, we proposed that EGCG oxides may have greater potential to regulate Notch signaling than EGCG. In this study, we isolated and identified EGCG oxides (compound **2**–**4**), using a chemical oxidation strategy, and evaluated for cytotoxicity against T-cell acute lymphoblastic leukemia cell line (HPB-ALL) by using the MTS assay. We found compound **3** significantly induced cell proliferation inhibition (38.3858 ± 1.67106 μM), cell apoptosis and cell cycle arrest in a dose-dependent manner. Remarkably, compound **3** inhibited expression of Notch1 compared with EGCG in HPB-ALL cells. Meanwhile, we found that compound **3** significantly inhibited c-Myc and Hes1, which are downstream target genes of Notch1. The findings demonstrate for the first time that an oxidation product of EGCG (compound **3**) inhibits T-cell acute lymphoblastic leukemia cell line (HPB-ALL) and is a promising agent for cancer therapy deserving further research.

Received 16th October 2019
Accepted 23rd December 2019

DOI: 10.1039/c9ra08459b

rsc.li/rsc-advances

1. Introduction

T-cell acute lymphoblastic leukemia (T-ALL) is an aggressive blood malignancy, which is usually reflected as an invasive tumor and accounts for approximately 25% and 15% of adult acute lymphoblastic leukemia in adult and pediatric cohorts, respectively.[1,2] Currently, T-ALL treatment schedules consist of high-dose chemotherapy, which is often associated with lack selectivity and displays significant toxic side effects.[3–5] There is an urgent clinical need for optimized treatment stratification and more effective antileukemic drugs for the treatment of human T-ALL. Development of targeted drugs, increase of tumor selectivity and decrease of toxicity are the key topics which are currently being studied.

Statistically, activating mutations in Notch1 occur in over 50% of T-ALLs,[6–8] The deregulated Notch signaling affects diverse cellular processes involved in growth, proliferation, apoptosis and cellular metabolism by driving the expression of c-Myc, Hes1 and regulating other critical oncogenic signaling pathways.[9–12] Many preclinical and clinical studies have explored the efficacy of targeting Notch in T-ALL, most commonly with γ-secretase inhibitors (GSIs).[13]

Natural products with various structures, unique biological activities and specific selectivity have served as important sources of lead compounds for antitumor agents which have been developed for clinical use.[14] (−)-Epigallocatechin-3-gallate (EGCG, **1**, Fig. 1) is the most abundant catechin (accounting for approximately 50% of total catechins) and has been reported to have stronger physiological activities.[15,16] Previously, some studies have reported that several proteins have been identified as EGCG direct interactors including the *trans*-membrane receptor 67LR, metalloproteinases (MMPs), Pin1 and TGFR-II13.[17] In addition, EGCG has the activity of regulating Notch signaling in the development of tumor angiogenesis and colorectal cancer.[18–21] However, the use of EGCG is often hindered by problems such as easy oxidation, ready degradation in aqueous solutions and the poor intestinal absorbance.[16,22]

There have been many studies reporting that EGCG encapsulated into nanocarriers leads to its strengthened stability and higher therapeutic effects.[23,24] In this study, we isolated and identified EGCG oxides by a chemical strategy, tested the ability

[a]*Key Laboratory of Pu-er Tea Science, Ministry of Education, Yunnan Agricultural University, Kunming, 650201, China. E-mail: shengj@ynau.edu.cn; wangxuanjun@gmail.com; zichengting@126.com*

[b]*College of Science, Yunnan Agricultural University, Kunming, 650201, China*

[c]*State Key Laboratory for Conservation and Utilization of Bio-Resources in Yunnan, Yunnan Agricultural University, Kunming, 650201, China*

† These authors contributed equally to this work.

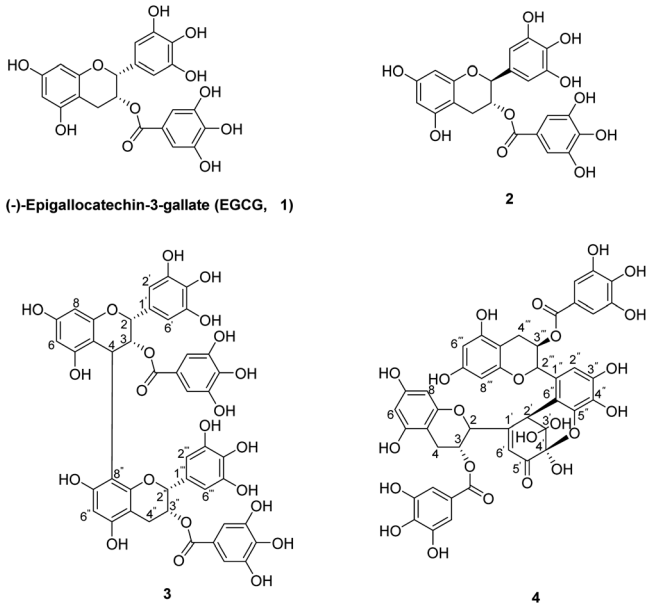

Fig. 1 The chemical structures of EGCG (**1**) and its oxides (**2–4**).

of oxides with EGCG to inhibit T-cell acute lymphoblastic leukemia cell line (HPB-ALL), and further developed more effective antileukemic drugs for the treatment of human T-ALL.

2. Results and discussion

2.1. Chemical oxidation and structural determination

The chemical oxidation of EGCG has been reported under various oxidative conditions, including $K_3[Fe(CN)_6]$,[25] $CuSO_4$,[26] and $CuCl_2$.[25] In this research, the oxidation of EGCG was based on X. C. Wan and R. G. Bailey *et al.* method[27,28] with some modification. EGCG was reacted with $K_3[Fe(CN)_6]/NaHCO_3$ at 25 °C for 15 min to yield the EGCG oxides **2–4** in 1.3–6.3% yields (Fig. 1).

Compound **2** was obtained as a white amorphous powder and shown to have the same molecular formula as EGCG by its HRESIMS. In the ^{1}H-NMR spectra (Table 1), the proton at C-2 (5.52 ppm, d, J = 2.4 Hz) and C-3 (4.96 ppm, d, J = 2.0 Hz) appear as a double peak, indicating a *cis*-relationship between H-2 and H-3. Compound **3** was isolated as a yellow amorphous powder. The negative HRESIMS at m/z 913.7339 $[M-H]^-$ (calcd

Table 1 ^{1}H-NMR and ^{13}C-NMR data for EGCG and EGCG oxides **2–4**

	EGCG (δ)		Compound **2** (δ)		Compound **3** (δ)		Compound **4** (δ)	
C position	δ_C	δ_H	δ_C	δ_H	δ_C	δ_H	δ_C	δ_H
2	78.6	5.56 (brs)	78.6	5.52 (d, J = 2.4 Hz)	76.3	5.23 (brs)	94.0	4.47 (s)
3	69.9	4.92 (s)	69.9	4.96 (d, J = 2.0 Hz)	69.0	4.90 (s)	69.3	4.47 (s)
4	26.8	3.03–2.92 (m, H)	26.8	3.02–2.90 (m, H)	26.9	4.72 (s)	27.1	3.16–3.12 (m, H)
5 (7)	157.8		157.9		157.7		157.7	
6	96.5	5.94 (s)	96.4	5.93 (s)	96.6	5.88 (s)	96.8	5.92 (d, J = 2.3 Hz)
8	95.9	5.94 (s)	95.8	5.93 (s)	95.9	5.87 (s)	95.8	5.90 (d, J = 2.3 Hz)
9	157.8		157.9		157.7		157.0	
10	99.4		99.4		99.0		99.7	
1′	130.8		130.7		129.5		156.5	
2′	106.9	6.49 (s)	106.8	6.48 (s)	108.3	6.74 (s)	54.9	3.34 (s)
3′	146.7		146.7		146.9		110.2	
4′	133.8		133.8		134.4		148.0	
5′	146.7		146.7		146.9		200.3	
6′	106.9	6.49 (s)	106.8	6.48 (s)	108.3	6.74 (s)	124.0	5.96 (s)
1″ (1‴)					129.5		128.0	
2″					76.3		109.2	6.42 (s)
3″					69.0	5.23–5.25 (m)	140.1	
4″					20.8	3.31–3.29 (m)	130.9	
5″					157.3		148.5	
6″					96.6	5.91 (d, J = 2.3 Hz)	114.9	
7″ (9″)					157.7			
8″ (8‴)					112.3		95.7	5.75 (d, J = 2.3 Hz)
10″ (10‴)					99.0		99.2	
2‴					108.3	6.74 (s)	78.5	5.45 (brs)
3‴					145.4		66.4	4.57 (s)
4‴					134.4		27.0	2.89–2.82 (m)
5‴ (7‴)					145.4		157.7	
6‴					108.3	6.74 (s)	96.6	5.80 (d, J = 2.3 Hz)
9‴							157.0	
Galloyl 0	167.7		167.6		167.8		167.7	
Galloyl 1	121.4		121.4		121.4		121.1	
Galloyl 2 (6)	110.2	6.94 (s, 2H)	110.2	6.93 (2H, s)	110.3	6.91 (s, 2H)	110.2	6.95 (s, 2H)
Galloyl 3 (5)	146.7		146.7		146.3		146.3	
Galloyl 4	139.8		139.7		139.8		139.8	

for $C_{44}H_{34}O_{22}$, 913.7340) supporting a molecular formula of $C_{44}H_{34}O_{22}$. The ^{1}H-NMR and ^{13}C-NMR spectra of compound **3** (Table 1) corresponded to the data reported in the literature.[29] Compounds **4**, a yellow amorphous powder, was assigned the molecular formula of $C_{44}H_{34}O_{23}$ determined by the negative HRESIMS at *m*/*z* 929.1450 $[M-H]^-$ (calcd for $C_{44}H_{34}O_{23}$, 929.1490), as well as from its NMR data (Table 1), which displayed a signal pattern similar to the data reported in the literatures.[30,31]

2.2. Compound 3 is identified as the most potent cytotoxic compound against HPB-ALL cells

We tested the stability of compounds with H_2O_2 quantitative assay kit. As shown in Fig. 2A, EGCG was oxidized significantly. However, the stability of the compound **2**, **3** and **4** was significantly improved compared with EGCG.

Previous studies have identified several T-ALL cell lines that are sensitive to GSI treatment.[6,32] To identify anticancer activity of EGCG oxides, we treated HPB-ALL cells with EGCG and its oxides in different concentrations and measured the cell viability using MTS assay (Fig. 2B). As shown in Fig. 2B, compound **3** appeared to be the most potent of these oxides. The IC_{50} value of compound **3** was 38.3858 ± 1.67106 μM in the HPB-ALL cells.

2.3. Compound 3 blocks Notch1 processing in HPB-ALL cells

Cell growth and proliferation can be regulated by Notch1 in T-ALL.[33] Previous studies have shown that EGCG regulates the inflammatory response by targeting Notch.[34,35] In addition, compound **3** is a dimeric EGCG derivative, share a similar chemical structure with EGCG. Therefore, we speculated that the cytotoxicity of compound **3** may be partly due to the inhibition of Notch1 signaling pathway. To investigate the effects of compound **3** on Notch1 signaling pathway, we examined the expression of Notch1 and the downstream proteins in HPB-ALL cells (Fig. 3). As shown in Fig. 3B–F, HPB-ALL cells were treated with compound **3** at the concentration of 5, 10, 20, 40, 60 μM for 12 h and the expression level of Notch1, cleaved-Notch1, c-Myc and Hes1 were significantly decreased.[7] Meanwhile, we also found that the expression of proliferation marker Ki67 was significantly reduced (Fig. 3B and G). These findings suggest that compound **3** inhibited the proliferation of HPB-ALL cells may be through down-regulating the expression of Notch1 and Ki67.

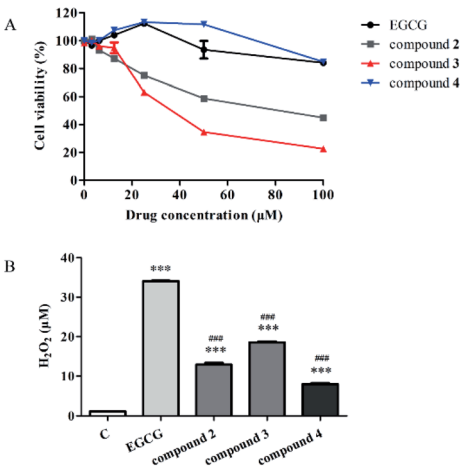

Fig. 2 The stability of compounds and the effects on the proliferation of HPB-ALL cells. (A) The HPB-ALL cells were treated with EGCG and compounds **2**–**4** (3.125, 6.25, 12.5, 25, 50 and 100 μM) for 48 h. Cell proliferation was measured by MTS assay. (B) The stability of compounds was assessed by determining the H_2O_2 content using a H_2O_2 quantitative assay kit. Data represent the average of three independent experiments (mean ± SEM). ***p < 0.001 *vs.* the control. ###p < 0.001 *vs.* EGCG.

2.4. Compound 3 induces cell cycle G2 arrest in HPB-ALL cells

Given that compound **3** inhibited HPB-ALL cells proliferation, we wondered whether **3** causes cell cycle arrest. We treated the HPB-ALL cells with compound **3** (5, 10, 20, 40, 60 μM) for 48 h and analyzed their cell cycle profiles by propidium iodide (PI) staining (Fig. 4). As shown in Fig. 4A and B, in the HPB-ALL cells, compound **3** significantly increased the percentage of cells in G2 phase compared to control. Meanwhile, we examined the protein levels of several cell cycle (CDK2, cyclin E, cyclin D1). As shown in Fig. 4C–F, compound **3** reduced the expression levels of CDK2 and cyclin E, increased the expression levels of cyclin D1.

2.5. Compound 3 induces apoptosis in HPB-ALL cells

Previous studies have shown that EGCG exhibits the potential to promote apoptosis of tumor cells.[36,37] Compound **3** has good

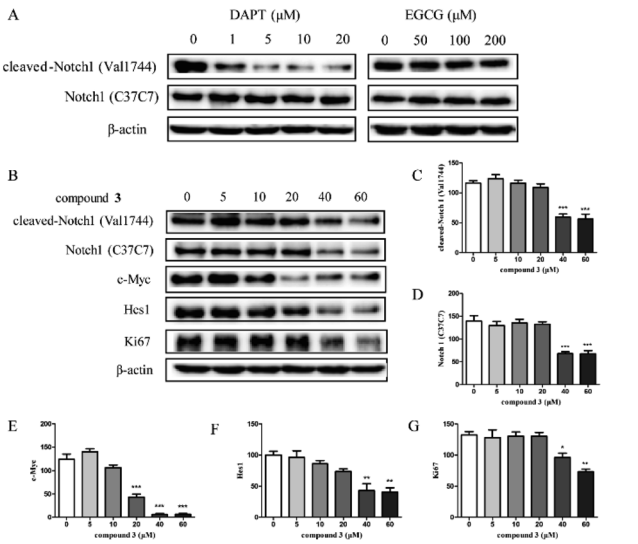

Fig. 3 The effect of compound **3** on Notch1 processing and downstream signaling pathway in HPB-ALL cells. (A) HPB-ALL cells were treated with DAPT (1, 5, 10, 20 μM), and EGCG (50, 100, 200 μM) for 12 h. (B) HPB-ALL cells were treated with compound **3** (5, 10, 20, 40, 60 μM) for 12 h. The expression levels by western blot (WB) to detect Notch1, cleaved-Notch1, c-Myc, Hes1 and Ki67. β-Actin was used as the loading control. (C–G) Quantification of relative cleaved-Notch1, Notch1, c-Myc and Hes1 protein levels. Data represent the average of three independent experiments (mean ± SEM). *p < 0.01, **p < 0.005, ***p < 0.001 *vs.* the control.

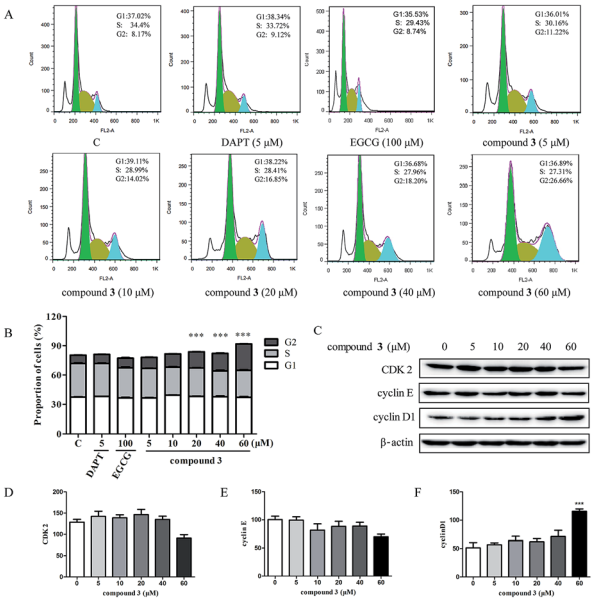

Fig. 4 Compound **3** induces cell cycle G2 arrest in HPB-ALL cells. (A) HPB-ALL cells were treated with DAPT (5 μM), EGCG (100 μM) and compound **3** (5, 10, 20, 40, 60 μM) for 48 h. The cell cycle distribution was analyzed by FlowJo software (version 7.6). (B) Quantification of the cell populations in each phase of the cell cycle was presented in HPB-ALL cells. (C) HPB-ALL cells were treated with compound **3** (5, 10, 20, 40, 60 μM) for 12 h. The protein levels of cell cycle-related protein were checked by western blot (WB). β-Actin was used as the loading control. (D–F) Quantification of relative CDK2, cyclin E and cyclin D1 protein levels. Data represent the average of three independent experiments (mean ± SEM). ***$p < 0.001$ *vs.* the control.

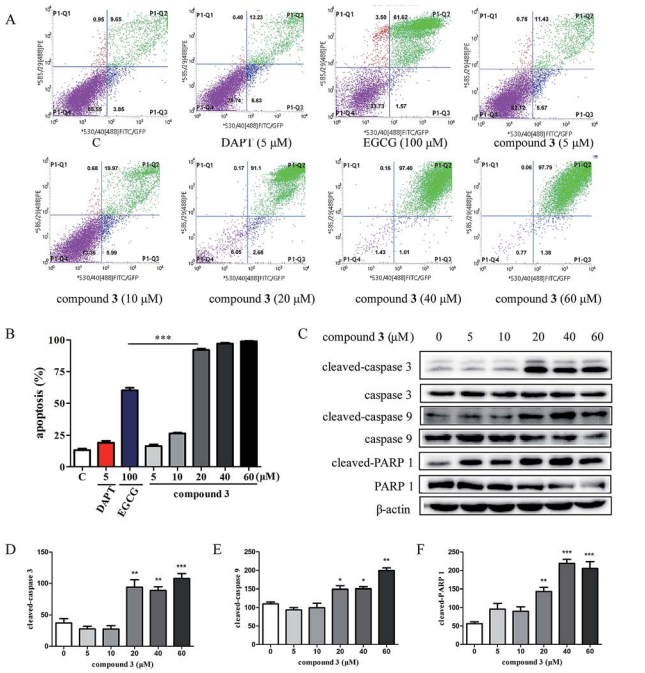

Fig. 5 Compound **3** induces apoptosis in HPB-ALL cells. (A) Flow cytometry of T-ALL cells HPB-ALL after treatment with DAPT (5 μM), EGCG (100 μM) and compound **3** (5, 10, 20, 40, 60 μM) for 48 h. (B) The ratio of apoptotic cells in each group are expressed as percentages. (C) The cells were treated with compound **3** (5, 10, 20, 40, 60 μM) for 12 h. The expression level of cleaved-caspase 3, caspase 3, cleaved-caspase 9, caspase 9, cleaved-PARP 1, and PARP 1 were detected by western blot (WB). β-Actin was used as the loading control. (D–F) Quantification of relative cleaved-caspase 3, cleaved-caspase 9 and cleaved-PARP 1 protein levels. Data represent the average of three independent experiments (mean ± SEM). *$p < 0.01$, **$p < 0.005$, ***$p < 0.001$ *vs.* the control.

cytotoxicity against HPB-ALL cell lines, suggesting that compound **3** mainly induces cell death in addition to causing cell cycle arrest. To test whether compound **3** induces apoptosis in HPB-ALL cells, we treated the cells with DAPT (5 μM), EGCG (100 μM) and compound **3** (5, 10, 20, 40, 60 μM) for 48 h, and measured the apoptosis of the HPB-ALL cells by FITC Annexin V staining and flow cytometry. Compound **3** significantly induced Annexin V positive apoptotic cells in HPB-ALL cells (Fig. 5A and B). Moreover, compound **3** induced the expression levels of caspase 3, caspase 9 and PARP 1, and increased the expression levels of cleaved-caspase 3, cleaved-caspase 9 and cleaved-PARP 1 (Fig. 5C–F).

3. Experimental

3.1. Materials and methods

(−)-Epigallocatechin-3-gallate was purchased from Chengdu Proifa Technology Development Co., Ltd (Chengdu, China); 3-(4,5-dimethylthiazol-2-yl)-5-(3-carboxymethoxyphenyl)-2-(4-sulfophenyl)-2*H*-tetrazolium, inner salt (MTS) purchased from Promega (Madison, WI, USA). H_2O_2 quantitative assay kit was provided by sangon biotech (Shanghai, China). HPB-ALL cell line were purchased from the American Type Culture Collection (ATCC, Manassas, Virginia, USA); antibodies against cleaved-Notch1, Notch1, Hes1, cleaved-caspase 3, caspase 3, cleaved-caspase 9, caspase 9, CDK2 and β-actin were obtained from Cell Signaling Technology (Beverly, MA, USA). Antibodies against c-Myc, cleaved-PARP1, PARP1 and Ki67 were obtained from Abcam (Lake Placid, NY, USA). Antibodies against cyclin E and cyclin D1 were obtained from Santa Cruz Biotechnology (Santa Cruz, CA, USA). All reagents were commercially available and used without further purification unless indicated otherwise. The melting points were measured by an X-4 melting point apparatus and were uncorrected. Mass spectra (MS) and high-resolution mass spectra (HRMS) data were recorded on an Agilent 6540 Q-Tof (ESIMS) (Agilent, California, USA). Proton nuclear magnetic resonance (^{1}H-NMR) and carbon-13 nuclear magnetic resonance (^{13}C-NMR) spectra were recorded on Bruker AVANCE III 500 MHz (Bruker BioSpin GmbH, Rheinstetten, Germany) instruments, using tetramethylsilane (TMS) as an internal standard: chemical shifts (δ) are given in ppm, coupling constants (J) in Hz, the solvent signals were used as references (CD_3OD: $\delta_C = 49.0$ ppm; residual CH_3OH in CD_3OD: $\delta_H = 4.78$ ppm). Silica gel (200–300 mesh) for column chromatography and silica GF_{254} for thin-layer chromatography (TLC) were produced by Qingdao Marine Chemical Company (China).

3.2. Oxidation of EGCG and characteristic data of compounds 2–4

To a solution of EGCG (200 mg, 0.45 mmol) in 10 mL of distilled water was added dropwise a solution of potassium hexacyanoferrate (III) (300 mg, 0.90 mmol) and solium hydrogen carbonate (100 mg, 1.2 mmol) in 10 mL of distilled water at 25 °C, pH 7.0 for 15 min. Then, the pH of resulting mixture was adjusted to 2.0 by addition of saturated aqueous citric acid (2 mL). The reaction mixture was extracted with ethyl acetate (10 mL × 3), and the combined organic layer was dried over sodium sulfate (s). The solvent was evaporated under vacuum and the residue was purified by column chromatography (silica gel, chloroform : methanol = 4 : 1 → 1 : 1, in 0.2% acetic acid) to afford compound **2** (4.9 mg, 2.5%), compound **3** (12.6 mg, 6.3%), and compound **4** (2.5 mg, 1.3%).

Compound **2**: white amorphous powder, ^{1}H-NMR (CD_3OD, 500 MHz) and ^{13}C-NMR (CD_3OD, 125 MHz) data: see Table 1; ESIMS: *m*/*z* 457 $[M-H]^-$, HRESIMS was calculated for $C_{22}H_{17}O_{11}$ $[M-H]^-$ 457.0849 and was found to be 457.0850. Compound **3**: yellow amorphous powder, ^{1}H-NMR (CD_3OD, 400 MHz) and ^{13}C-NMR (CD_3OD, 100 MHz) data: see Table 1; ESIMS: *m*/*z* 457 $[M-H]^-$, HRESIMS was calculated for $C_{44}H_{33}O_{22}$ $[M-H]^-$ 913.7340 and was found to be 913.7339. Compound **4**: yellow amorphous powder, ^{1}H-NMR (CD_3OD, 500 MHz) and ^{13}C-NMR (CD_3OD, 125 MHz) data: see Table 1; ESIMS: *m*/*z* 457 $[M-H]^-$, HRESIMS was calculated for $C_{44}H_{33}O_{23}$ $[M-H]^-$ 929.1490 and was found to be 929.1450.

3.3. Measurement of the stability of compounds

The medium containing the different compounds (50 μM) was incubated at 37 °C for 30 min. According to the instructions, the medium and operating fluid was transferred into a 96-well plate. The plate was shaken for 30 s and left at room temperature for 20 min. The optical density (OD) values were measured at 595 nm with a Flex Station 3 Multi-Mode Microplate Reader (Molecular Devices).

3.4. Cell toxicity assay

HPB-All cells were placed into 96-well plates at a density of 2.0×10^5 cells per well and treated with medium free of phenol red and different concentrations of EGCG and EGCG oxides. Cells was incubated at 37 °C for 48 h. 20 μL of MTS solution was transferred to each well, and then the plate was incubated at 37 °C for 4 h. The OD values were measured at 490 nm with Flex Station 3 Multi-Mode Microplate Reader (Molecular Devices).

3.5. Western blot analysis

HPB-ALL cells were seeded in the 100 mm plates at a density of 6.0×10^6 cells per well and treated with compound **3** at different concentrations in cell culture flasks, and then the cells were harvested and lysed in lysis buffer to assess the expression of Notch1, c-Myc, Hes1, caspase 3, caspase 9, PARP 1, Ki67, cyclin E, cyclin D1 and CDK2. Extracted proteins samples were quantified using bicinchoninic acid (BCA) assays; equal amounts were loaded 8% SDS-polyacrylamide gel and then transferred onto polyvinylidene fluoride (PVDF) membranes (EMD Millipore Corporation, Merck Life Sciences, KGaA, Darmstadt, Germany). Membranes containing protein blots were blocked with 5% non-fat milk in TBST at room temperature for 1 h and then incubated with the primary antibodies at 4 °C overnight. Following a wash with TBST, membranes were incubated with secondary antibodies for 1 h. Detection was performed using a FluorChem E System (ProteinSimple, Santa Clara, CA, United States).

3.6. Cell cycle analysis

HPB-ALL cells were seeded in the 6-well plates at a density of 1.0×10^6 cells per well, harvested, and washed twice with PBS. After The cells were synchronized for 48 h in medium containing 3% FBS in the presence or absence of DAPT, EGCG and compound **3**, and then washed in ice-cold PBS and fixed in 70% ethanol at 4 °C for 24 h. Then the cells were washed twice with cold PBS and stained in buffer containing PI (10 μg mL^{-1}) and RNase. After 30 min incubation in the dark on ice, cell cycle distributions were detected and analyzed by flow cytometry (BD FACSCalibur, USA).

3.7. Cell apoptosis assay

HPB-ALL cells were seeded in the 6-well plates at a density of 1.0×10^6 cells per well. After the cells were pretreated with DAPT, EGCG and compound **3** and incubated for 48 h in medium containing 3% FBS. Following collection and suspension in binding buffer, the cells were incubated with 5 μL of Annexin V and 5 μL of PI (BD Biosciences) for 15 minutes in darkness. Detection was performed using a flow cytometry (BD FACSJazz TM Cell Sorter, 655487, USA).

4. Conclusions

In summary, we isolated and identified EGCG oxides (compound **2–4**), using a chemical oxidation strategy, and evaluated for cytotoxicity against T-cell acute lymphoblastic leukemia cell line (HPB-ALL) by using MTS assay. Among them, compound **3** showed the highest anticancer activity with its IC_{50} values at 38.3858 ± 1.67106 μM. We founding that compound **3** inhibited the proliferation of HPB-ALL cells may be through down-regulating the expression of Notch1 and Ki67. Compound **3** induced cell cycle G2 arrest in HPB-ALL cells, and also induced the expression levels of the apoptotic maker protein (caspase 3, caspase 9 and PARP 1). We demonstrated for the first time that an oxidation product of EGCG (compound **3**) inhibits T-cell acute lymphoblastic leukemia cell line HPB-ALL *via* the regulation of Notch1 expression.

Conflicts of interest

The authors declare no conflict of interest.

Acknowledgements

We are grateful to the National Nature Science Foundation of China for financial support (No. 21602196); the Yunnan Provincial Science and Technology Department (No. 2017ZF003, 2017FD084, and 2017FG001-046).

Notes and references

1 A. A. Ferrando, D. S. Neuberg, J. Staunton, M. L. Loh, C. Huard and S. C. Raimondi, *Cancer Cell*, 2002, **1**, 75–87.
2 E. Baghbani, B. Baradaran, F. Pak, L. Mohammadnejad, D. Shanehbandi, B. Mansoori, V. Khaze, N. Montazami, A. Montazami and P. Kokhaei, *Biomed. Pharmacother.*, 2017, **86**, 41–47.
3 A. J. Barrett, M. M. Horowitz, B. H. Pollock, M. J. Zhang, M. M. Bortin and G. R. Buchanan, *N. Engl. J. Med.*, 1994, **331**, 1253–1258.
4 J. M. Goldberg, L. B. Silverman, D. E. Levy, V. K. Dalton, R. D. Gelber and L. Lehmann, *J. Clin. Oncol.*, 2003, **21**, 3616–3622.
5 P. V. Vlierberghe and A. Ferrando, *J. Clin. Invest.*, 2012, **122**, 3398–3406.
6 A. P. Weng, A. A. Ferrando, L. Woojoong, J. P. Morris, L. B. Silverman and S. I. Cheryll, *Science*, 2004, **306**, 269–271.
7 C. Grabher, H. Von Boehmer and A. T. Look, *Nat. Rev. Cancer*, 2006, **6**, 347–359.
8 I. Pinto, M. Duque, J. Gonçalves, P. Akkapeddi, M. L. Oliveira, R. Cabrita, J. A. Yunes, S. K. Durum, J. T. Barata and R. Fragoso, *Oncogene*, 2019, 1–12.
9 V. Giambra, C. R. Jenkins, H. Wang, S. H. Lam, O. O. Shevchuk and O. Nemirovsky, *Nat. Med.*, 2012, **18**, 1693–1698.
10 S. Jarriault, B. O. Le, E. Hirsinger, O. Pourquié, F. Logeat and C. F. Strong, *Mol. Cell. Biol.*, 1998, **18**, 7423–7431.
11 S. Weijzen, P. Rizzo, M. Braid, R. Vaishnav, S. M. Jonkheer, A. Zlobin, B. A. Osborne, S. Gottipati, J. C. Aster, W. C. Hahn, M. Rudolf, K. Siziopikou, W. M. Kast and L. Miele, *Nat. Med.*, 2002, **8**, 979–986.
12 A. P. Wen, *Genes Dev.*, 2006, **20**, 2096–2109.
13 N. Takebe, D. Nguyen and S. X. Yang, *Pharmacol. Ther.*, 2014, **141**, 140–149.
14 C. T. Zi, Y. S. Gao, L. Yang, S. Y. Feng, Y. Huang, L. Sun, Y. Jin, F. Q. Xu, F. W. Dong, Y. Li, Z. T. Ding, J. Zhou, Z. H. Jiang, S. T. Yuan and J. M. Hu, *Front. Chem.*, 2019, **7**, 434.
15 C. Cabrera, R. Gimenez and M. C. Lopez, *J. Agric. Food Chem.*, 2003, **51**, 4427–4435.
16 X. Zhang, J. Wang, J. M. Hu, Y. W. Huang, X. Y. Wu, C. T. Zi, X. J. Wang and J. Sheng, *Molecules*, 2016, **21**, 620.
17 A. Negri, V. Naponelli, F. Rizzi and S. Bettuzzi, *Nutrients*, 2018, **10**, 1–24.
18 L. T. Gu, J. Yang, S. Z. Su, W. W. Liu, Z. G. Shi and Q. R. Wang, *Neurochem. Res.*, 2015, **40**, 1211–1219.
19 H. Xie, J. Q. Sun, Y. Q. Chen, M. Zong, S. J. Li and Y. Wang, *Oxid. Med. Cell. Longevity*, 2015, **2015**, 1–10.
20 Y. Gao, G. O. Rankin, Y. Tu and Y. C. Chen, *Int. J. Oncol.*, 2016, **48**, 281–292.
21 H. Jin, W. Gong, C. Zhang and S. Wang, *OncoTargets Ther.*, 2013, **6**, 145–153.
22 S. Kitao, T. Matsudo, M. Sasaki, T. Horiuchi and H. Sekine, *Biosci. Biotechnol. Biochem.*, 1995, **59**, 2167–2169.
23 O. Krupkova, S. J. Ferguson and K. Wuertz-Kozak, *J. Nutr. Biochem.*, 2016, **37**, 1–12.
24 G. Andreia, I. Frias, N. A. Neves, M. Pinheiro and S. Reis, *BioMed Res. Int.*, 2017, **2017**, 1–15.
25 Y. Takino, H. Imagawa, Y. Aoki and T. ocirc ko Ozawa, *Agric. Biol. Chem.*, 1963, **27**, 562–568.
26 T. Shii, M. Miyamoto, Y. Matsuo, T. Tanaka and I. Kouno, *Chem. Pharm. Bull.*, 2011, **59**, 1183–1185.
27 X. C. Wan, H. E. Nursten, C. Ya, A. L. Davis, J. P. G. Wilkins and A. P. Davies, *J. Sci. Food Agric.*, 1997, **74**, 401–408.
28 R. G. Bailey, H. E. Nursten and I. Mcdowell, *J. Sci. Food Agric.*, 1993, **63**, 455–464.
29 J. P. de Mello, F. Petereit and A. Nahrstedt, *Phytochemistry*, 1996, **41**, 807–813.
30 S. Valcic, A. Muders, N. E. Jacobsen, D. C. Liebler and B. N. Timmermann, *Chem. Res. Toxicol.*, 1999, **12**, 382–386.
31 T. Tanaka, S. Watarumi, Y. Matsuo, M. Kamei and I. Kouno, *Tetrahedron*, 2003, **59**, 39–47.
32 T. Palomero, M. L. Sulis, M. Cortina, P. J. Real, K. Barnes, M. Ciofani, E. Caparros, J. Buteau, K. Brown, S. L. Perkins, G. Bhagat, A. M. Agarwal, G. Basso, M. Castillo, S. Nagase, C. Cordon-Cardo, R. Parsons, J. C. Zúñiga-Pflücker, M. Dominguez and A. Ferrando, *Nat. Med.*, 2007, **13**, 1203–1210.
33 M. Paganin and A. Ferrando, *Blood Rev.*, 2011, **25**, 83–90.
34 T. F. Wang, Z. M. Xiang, Y. Wang, X. Li, C. Y. Fang, S. Song, C. L. Li, H. S. Yu, H. Wang, L. Yan, S. M. Hao, X. J. Wang and J. Sheng, *Front. Immunol.*, 2017, **8**, 433.
35 Y. W. Huang, Q. Q. Zhu, X. Y. Yang, H. H. Xu, B. Sun, X. J. Wang and J. Sheng, *FASEB J.*, 2018, **33**, 1–12.
36 W. H. Yang, Y. C. Fong, C. Y. Lee, T. R. Jin, J. T. Tzen, T. M. Li and C. H. Tang, *J. Cell. Biochem.*, 2011, **112**, 1601–1611.
37 Y. Q. Wang, J. L. Lu, Y. R. Liang and Q. S. Li, *Molecules*, 2018, **23**, 23–34.

